

A NOTE ON THE SPECTRAL ANALYSIS OF MATRIX SEQUENCES VIA GLT MOMENTARY SYMBOLS: FROM ALL-AT-ONCE SOLUTION OF PARABOLIC PROBLEMS TO DISTRIBUTED FRACTIONAL ORDER MATRICES*

MATTHIAS BOLTEN*, SVEN-ERIK EKSTRÖM†, ISABELLA FURCI*, AND
STEFANO SERRA-CAPIZZANO‡

Abstract. The first focus of this paper is the characterization of the spectrum and the singular values of the coefficient matrix stemming from the discretization of a parabolic diffusion problem using a space-time grid and secondly from the approximation of distributed-order fractional equations. For this purpose we use the classical GLT theory and the new concept of GLT momentary symbols. The first permits us to describe the singular value or eigenvalue asymptotic distribution of the sequence of the coefficient matrices. The latter permits us to derive a function that describes the singular value or eigenvalue distribution of the matrix of the sequence, even for small matrix sizes, but under given assumptions. The paper is concluded with a list of open problems, including the use of our machinery in the study of iteration matrices, especially those concerning multigrid-type techniques.

Key words. Toeplitz matrices, asymptotic distribution of eigenvalues and singular values, numerical solution of discretized equations for boundary value problems involving PDEs, fractional differential equations

AMS subject classifications. 15B05, 34L20, 65N22, 35R11

1. Introduction and notation. As it is well known, many practical applications require to numerically solve linear systems of Toeplitz kind and of large dimensions. As a consequence, a number of iterative techniques such as preconditioned Krylov methods, multigrid procedures, and sophisticated combinations of them have been designed (see [10, 27] and the references therein). Linear systems with Toeplitz coefficient matrices of large dimension arise when dealing with the numerical solution of (integro-)differential equations and of problems with Markov chains. More recently, new examples of such applications to real-world problems have emerged. The first focus of this paper is the characterization of the spectrum and the singular values of the coefficient matrix stemming from the discretization of a parabolic diffusion problem using a space-time grid. More specifically, we consider the diffusion equation in one space dimension,

$$u_t = u_{xx}, \quad x \in (a, b), \quad t \in [0, T],$$

and we approximate our parabolic model problem on a rectangular space-time grid consisting of N_t time intervals and N_x space intervals.

The second focus concerns the matrix sequences involved with the discretization of distributed-order fractional differential equations (FDEs), which have gained a lot of attention. Owing to the nonlocal nature of fractional operators, independently of the locality of the approximation methods, the matrix structures are dense, and, under assumptions of uniform step-sizing and of constant coefficients in the involved operators, the matrices are again of Toeplitz type (unilevel, or multilevel according to the dimensionality of the considered spatial domains).

*Received March 2, 2022. Accepted December 1, 2022. Published online on January 30, 2023. Recommended by Silvia Noschese.

*Bergische Universität Wuppertal, Department of Mathematics and Computer Science, Gaußstraße 20, 42119 Wuppertal, Germany. (bolten, furci@uni-wuppertal.de).

†Uppsala University, Department of Information Technology, Lägerhyddsv. 1, SE-751 05, Uppsala, Sweden (sven-erik.ekstrom@it.uu.se).

‡University of Insubria, Department of Science and High Technology, via Valleggio 11, 22100, Como, Italy (s.serracapizzano@uninsubria.it).

When the fractional order is fixed, the spectral analysis of such matrices (conditioning, extremal eigenvalues, ...) can be performed by exploiting the well-established analysis of the spectral features of Toeplitz matrix sequences generated by Lebesgue-integrable functions and the more recent Generalized Locally Toeplitz (GLT) theory [23]; see for instance [17, 18]. However, in the case of the numerical approximation of distributed-order fractional operators, also the spectral analysis of the resulting matrices is more involved. We recall that distributed-order FDEs can be interpreted as a parallel distribution of derivatives of fractional orders, whose most immediate application consists of the physical modeling of systems characterized by a superposition of different processes operating in parallel. As an example, we mention the application of fractional distributed-order operators as a tool for accounting memory effects in composite materials [13] or multi-scale effects [11]. For a detailed review on the topic we refer the reader to [16].

In order to study the involved structured linear systems of both integral and differential equations, we will use the classical theory of GLT matrix sequences [23, 24] and the new concept of GLT momentary symbols. The first permits us to describe the singular value or eigenvalue asymptotic distribution of a sequence of coefficient matrices; the latter permits us to derive a function which describes the singular value or eigenvalue distribution of a fixed matrix of the sequence, even for small matrix sizes, under given assumptions.

This paper is organized as follows. The remaining part of this section is devoted to definitions, notation, and the necessary background for our analysis: in particular we provide a formal definition of GLT momentary symbols. Section 2 is devoted to setting up the problem and to derive the relevant matrix structures. The distributional analysis both for the eigenvalues and singular values is the main focus of Section 2.3, while Section 3 contains similar results for specific matrix structures with generating function depending on the matrix size and which arise in the context of fractional differential equations with distributed orders. Section 4 contains conclusions and a list of open problems, including the use of our machinery in the study of iteration matrices, especially those concerning multigrid-type techniques.

1.1. Background and definitions. Throughout this paper we use the following notations. Letting $f : G \rightarrow \mathbb{C}$ be a function belonging to $L^1(G)$, with $G \subseteq \mathbb{R}^\ell$, $\ell \geq 1$, a measurable set, we denote by $\{A_n\}_n$ the matrix sequence whose elements are given by the matrices A_n of dimension $n \times n$. Letting $s, d \in \mathbb{N}$, $\mathbf{n} = (n_1, n_2, \dots, n_d)$ be a multi-index, we indicate by $\{A_{\mathbf{n}}\}_{\mathbf{n}}$, the d -level $s \times s$ block matrix sequence whose elements are the matrices $A_{\mathbf{n}}$ of size $d = d(\mathbf{n}, s) = sn_1n_2 \cdots n_d$.

1.2. Toeplitz and circulant matrix sequences. In the following we report the main background concerning the concepts of Toeplitz and circulant matrices, for simplicity in the scalar unilevel setting. We only provide the generalization in the block multilevel case of the results that will be exploited for the purpose of the paper.

DEFINITION 1.1. An $n \times n$ Toeplitz matrix A_n is a matrix that has equal entries along each diagonal and can be written as

$$A_n = [a_{i-j}]_{i,j=1}^n = \begin{bmatrix} a_0 & a_{-1} & a_{-2} & \cdots & \cdots & a_{1-n} \\ a_1 & \ddots & \ddots & \ddots & \ddots & \vdots \\ a_2 & \ddots & \ddots & \ddots & \ddots & \vdots \\ \vdots & \ddots & \ddots & \ddots & \ddots & a_{-2} \\ \vdots & \ddots & \ddots & \ddots & \ddots & a_{-1} \\ a_{n-1} & \cdots & \cdots & a_2 & a_1 & a_0 \end{bmatrix}, \quad a_k \in \mathbb{C}, \quad k = 1-n, \dots, n-1.$$

In the following we focus on the two important subclasses given by the Toeplitz matrices $T_n(f) \in \mathbb{C}^{n \times n}$ and the circulant matrices $C_n(f) \in \mathbb{C}^{n \times n}$ associated with a function f , called the *generating function*.

DEFINITION 1.2. *Given f belonging to $L^1([-\pi, \pi])$ and periodically extended to the whole real line, the matrix $T_n(f)$ is defined as*

$$T_n(f) = \left[\hat{f}_{i-j} \right]_{i,j=1}^n,$$

where

$$(1.1) \quad \hat{f}_k := \frac{1}{2\pi} \int_{-\pi}^{\pi} f(\theta) e^{-ki\theta} d\theta, \quad k \in \mathbb{Z}, \quad i^2 = -1,$$

are the Fourier coefficients of f and

$$f(\theta) = \sum_{k=-\infty}^{\infty} \hat{f}_k e^{ki\theta},$$

is the Fourier series of f .

DEFINITION 1.3. *Let the Fourier coefficients of a given function $f \in L^1([-\pi, \pi])$ be defined as in formula (1.1). Then we define the $n \times n$ circulant matrix $C_n(f)$ associated with f as*

$$(1.2) \quad C_n(f) = \sum_{j=-(n-1)}^{n-1} \hat{a}_j Z_n^j = \mathbb{F}_n D_n(f) \mathbb{F}_n^*,$$

where $*$ denotes the transpose conjugate and Z_n is the $n \times n$ matrix defined by

$$(Z_n)_{ij} = \begin{cases} 1, & \text{if } i - j \equiv 1 \pmod{n}, \\ 0, & \text{otherwise.} \end{cases}$$

Moreover,

$$D_n(f) = \text{diag} (s_n(f(\theta_{j,n}^c))), \quad j = 1, \dots, n,$$

where

$$\theta_{j,n}^c = \frac{(j-1)2\pi}{n}, \quad j = 1, \dots, n,$$

and $s_n(f(\theta))$ is the n th Fourier sum of f given by

$$s_n(f(\theta)) = \sum_{k=1-n}^{n-1} \hat{f}_k e^{ki\theta}.$$

The matrix \mathbb{F}_n is the so-called Fourier matrix of order n , given by

$$(\mathbb{F}_n)_{i,j} = \frac{1}{\sqrt{n}} e^{i(i-1)\theta_{j,n}^c}, \quad i, j = 1, \dots, n.$$

In the case of the Fourier matrix, we have $\mathbb{F}_n \mathbb{F}_n^* = \mathbb{I}_n$, that is, \mathbb{F}_n is complex-symmetric and unitary with \mathbb{I}_n being the identity matrix of size n .

TABLE 1.1
Different types of generating function and the associated Toeplitz matrix.

Type of generating function		Associated Toeplitz matrix
univariate scalar	$f(\theta) : [-\pi, \pi] \rightarrow \mathbb{C}$	unilevel scalar $T_n(f) \in \mathbb{C}^{n \times n}$
d -variate scalar	$f(\boldsymbol{\theta}) : [-\pi, \pi]^d \rightarrow \mathbb{C}$	d -level scalar $T_{\mathbf{n}}(f) \in \mathbb{C}^{d(\mathbf{n},1) \times d(\mathbf{n},1)}$
univariate matrix-valued	$\mathbf{f}(\theta) : [-\pi, \pi] \rightarrow \mathbb{C}^{s \times s}$	unilevel block $T_n(\mathbf{f}) \in \mathbb{C}^{d(\mathbf{n},s) \times d(\mathbf{n},s)}$
d -variate matrix-valued	$\mathbf{f}(\boldsymbol{\theta}) : [-\pi, \pi]^d \rightarrow \mathbb{C}^{s \times s}$	d -level block $T_{\mathbf{n}}(\mathbf{f}) \in \mathbb{C}^{d(\mathbf{n},s) \times d(\mathbf{n},s)}$

The proof of the second equality in (1.2), which implies that the columns of the Fourier matrix \mathbb{F}_n are the eigenvectors of $C_n(f)$, can be found in [23, Theorem 6.4]. Note that from the definition it follows that, if f is a trigonometric polynomial of fixed degree less than n , then the entries of $D_n(f)$ are the eigenvalues of $C_n(f)$, explicitly given by sampling the generating function f using the grid $\theta_{j,n}^c$:

$$\begin{aligned} \lambda_j(C_n(f)) &= f(\theta_{j,n}^c), & j &= 1, \dots, n, \\ D_n(f) &= \text{diag}(f(\theta_{j,n}^c)), & j &= 1, \dots, n. \end{aligned}$$

The type of domain (either one-dimensional $[-\pi, \pi]$ or d -dimensional $[-\pi, \pi]^d$) and codomain (either the complex field or the space of $s \times s$ complex matrices) of f gives rise to different kinds of Toeplitz matrices; see Table 1.1 for a complete overview.

In particular, we provide the definition of a d -level $s \times s$ block Toeplitz matrices $T_{\mathbf{n}}(\mathbf{f})$ starting from d -variate matrix-valued function $\mathbf{f} : [-\pi, \pi]^d \rightarrow \mathbb{C}^{s \times s}$ with $\mathbf{f} \in L^1([-\pi, \pi]^d)$.

DEFINITION 1.4. *Given a function $\mathbf{f} : [-\pi, \pi]^d \rightarrow \mathbb{C}^{s \times s}$, its Fourier coefficients are given by*

$$\hat{\mathbf{f}}_{\mathbf{k}} := \frac{1}{(2\pi)^d} \int_{[-\pi, \pi]^d} \mathbf{f}(\boldsymbol{\theta}) e^{-i\langle \mathbf{k}, \boldsymbol{\theta} \rangle} d\boldsymbol{\theta} \in \mathbb{C}^{s \times s}, \quad \mathbf{k} = (k_1, \dots, k_d) \in \mathbb{Z}^d,$$

where $\boldsymbol{\theta} = (\theta_1, \dots, \theta_d)$, $\langle \mathbf{k}, \boldsymbol{\theta} \rangle = \sum_{i=1}^d k_i \theta_i$, and the integrals of matrices are computed elementwise. The associated generating function can be defined via its Fourier series as

$$\mathbf{f}(\boldsymbol{\theta}) = \sum_{\mathbf{k} \in \mathbb{Z}^d} \hat{\mathbf{f}}_{\mathbf{k}} e^{i\langle \mathbf{k}, \boldsymbol{\theta} \rangle}.$$

The d -level $s \times s$ block Toeplitz matrix associated with \mathbf{f} is the matrix of dimension $d(\mathbf{n}, s)$, with $\mathbf{n} = (n_1, \dots, n_d)$, given by

$$T_{\mathbf{n}}(\mathbf{f}) = \sum_{\mathbf{e}-\mathbf{n} \leq \mathbf{k} \leq \mathbf{n}-\mathbf{e}} T_{n_1}(e^{ik_1\theta_1}) \otimes \dots \otimes T_{n_d}(e^{ik_d\theta_1}) \otimes \hat{\mathbf{f}}_{\mathbf{k}},$$

where \mathbf{e} is the vector of all ones and where $\mathbf{s} \leq \mathbf{t}$ means that $s_j \leq t_j$ for any $j = 1, \dots, d$.

DEFINITION 1.5. *If $\mathbf{n} \in \mathbb{N}^d$ and $\mathbf{a} : [0, 1]^d \rightarrow \mathbb{C}^{s \times s}$, we define the \mathbf{n} th d -level and $s \times s$ block diagonal sampling matrix as the following multilevel block diagonal matrix of dimension $d(\mathbf{n}, s)$:*

$$D_{\mathbf{n}}(\mathbf{a}) = \text{diag}_{\mathbf{e} \leq \mathbf{j} \leq \mathbf{n}} \mathbf{a} \left(\frac{\mathbf{j}}{\mathbf{n}} \right),$$

where we recall that $\mathbf{e} \leq \mathbf{j} \leq \mathbf{n}$ means that \mathbf{j} varies from \mathbf{e} to \mathbf{n} , that is, $1 \leq j_k \leq n_k$ for all $k = 1, \dots, d$. Furthermore, in assembling the matrix $D_{\mathbf{n}}(\mathbf{a})$, the lexicographic ordering is used. More precisely, like the digits of a d -digit number smaller than 1 in a given basis, the

quantity j_d moves fastest, j_{d-1} second fastest, and so on till j_1 , which moves slowest. If $d = 2$ and $n_1 = 2$, $n_2 = 4$, then the ordering is the following: $(1, 1)$, $(1, 2)$, $(1, 3)$, $(1, 4)$, $(2, 1)$, $(2, 2)$, $(2, 3)$, $(2, 4)$.

The following result provides an important relation between tensor products and multilevel Toeplitz matrices.

LEMMA 1.6 ([24]). Let $f_1, \dots, f_d \in L^1([-\pi, \pi])$, $\mathbf{n} = (n_1, n_2, \dots, n_d) \in \mathbb{N}^d$. Then,

$$T_{n_1}(f_1) \otimes \dots \otimes T_{n_d}(f_d) = T_{\mathbf{n}}(f_1 \otimes \dots \otimes f_d),$$

where the Fourier coefficients of $f_1 \otimes \dots \otimes f_d$ are given by

$$(f_1 \otimes \dots \otimes f_d)_{\mathbf{k}} = (f_1)_{k_1} \dots (f_d)_{k_d}, \quad \mathbf{k} \in \mathbb{Z}^d.$$

1.3. Asymptotic distributions. In this section we introduce the definition of *asymptotic distribution* in the sense of the eigenvalues and of the singular values, first for a generic matrix sequence $\{A_n\}_n$, and then we report specific results concerning the distributions of Toeplitz and circulant matrix sequences. Finally, we recall the notion of the GLT algebra, and we introduce a general notion of GLT momentary symbols. We remind that, in a more specific and limited setting, the notion of momentary symbols is given in [7]: here we generalize the definition in [7].

DEFINITION 1.7 ([23, 24, 25, 33]). Let $f, \mathfrak{f} : G \rightarrow \mathbb{C}$ be measurable functions, defined on a measurable set $G \subset \mathbb{R}^\ell$, with $\ell \geq 1$, $0 < \mu_\ell(G) < \infty$. Let $\mathcal{C}_0(\mathbb{K})$ be the set of continuous functions with compact support over $\mathbb{K} \in \{\mathbb{C}, \mathbb{R}_0^+\}$, and let $\{A_n\}_n$ be a sequence of matrices with eigenvalues $\lambda_j(A_n)$, $j = 1, \dots, d_n$, and singular values $\sigma_j(A_n)$, $j = 1, \dots, d_n$. Then:

- The matrix sequence $\{A_n\}_n$ is distributed as f in the sense of the **singular values** and we write

$$\{A_n\}_n \sim_\sigma f,$$

if the following limit relation holds for all $F \in \mathcal{C}_0(\mathbb{R}_0^+)$:

$$(1.3) \quad \lim_{n \rightarrow \infty} \frac{1}{d_n} \sum_{j=1}^{d_n} F(\sigma_j(A_n)) = \frac{1}{\mu_\ell(G)} \int_G F(|f(\boldsymbol{\theta})|) d\boldsymbol{\theta}.$$

The function f is called the **singular value symbol**, which asymptotically describes the singular value distribution of the matrix sequence $\{A_n\}_n$.

- The matrix sequence $\{A_n\}_n$ is distributed as \mathfrak{f} in the sense of the **eigenvalues** and we write

$$\{A_n\}_n \sim_\lambda \mathfrak{f},$$

if the following limit relation holds for all $F \in \mathcal{C}_0(\mathbb{C})$:

$$(1.4) \quad \lim_{n \rightarrow \infty} \frac{1}{d_n} \sum_{j=1}^{d_n} F(\lambda_j(A_n)) = \frac{1}{\mu_\ell(G)} \int_G F(\mathfrak{f}(\boldsymbol{\theta})) d\boldsymbol{\theta}.$$

The function \mathfrak{f} is called the **eigenvalue symbol**, which asymptotically describes the eigenvalue distribution of the matrix sequence $\{A_n\}_n$.

REMARK 1.8. Note that, if A_n is normal for any n or at least definitely, then $\{A_n\}_n \sim_\sigma f$ and $\{A_n\}_n \sim_\lambda \mathfrak{f}$ imply that $f = \mathfrak{f}$. Of course this is true for Hermitian Toeplitz matrix sequences as emphasized in Theorem 1.9 and Theorem 1.10.

Moreover, considering the case $d = 1$, if f (or \mathbf{f}) is smooth enough, then the informal interpretation of the limit relation (1.3) (or (1.4)) is that, for n sufficiently large, the n singular values (or eigenvalues) of A_n can be approximated by a sampling of $|f(\theta)|$ (or $\mathbf{f}(\theta)$) on an equispaced grid of the interval G , up to the presence of possibly $o(n)$ outliers. It is worthwhile to notice that in most of the Toeplitz and PDE/FDE applications, the number of actual outliers is often limited to $O(1)$ with often a small number of outliers (see [4, 3, 23, 24] and the references therein).

The generalization of Definition 1.7 and Remark 1.8 to the block setting and multilevel block setting can be found in [4, 3] and in the references therein. In the case where the matrix sequence is a Toeplitz matrix sequence generated by a function, the singular value distribution and the spectral distribution have been well studied in the past few decades. In this respect, the seminal work is that of Szegő reported in the book [25], where it is shown that the eigenvalues of the Toeplitz matrices $T_n(f)$ generated by a real-valued $f \in L^\infty([-\pi, \pi])$ are asymptotically distributed as f . Moreover, under the same assumption on f , Avram and Parter [2, 28] proved that the singular values of $T_n(f)$ are distributed as $|f|$. This result has been undergone many generalizations and extensions over the years (see [4, 3, 23, 24] and the references therein).

The generalized Szegő theorem that describes the singular value and spectral distribution of Toeplitz sequences generated by a scalar $f \in L^1([-\pi, \pi])$ is given as follows [34]:

THEOREM 1.9. *Suppose that $f \in L^1([-\pi, \pi])$. Let $T_n(f)$ be the Toeplitz matrix generated by f . Then we have*

$$\{T_n(f)\}_n \sim_\sigma f.$$

Moreover, if f is real-valued almost everywhere (a.e.), then

$$\{T_n(f)\}_n \sim_\lambda f.$$

Tilli [32] generalized the proof to the block-Toeplitz setting, and we report the extension of the eigenvalue result to the case of multivariate Hermitian matrix-valued generating functions.

THEOREM 1.10. *Suppose that $\mathbf{f} : [-\pi, \pi]^d \rightarrow \mathbb{C}^{s \times s}$, $\mathbf{f} \in L^1([-\pi, \pi]^d)$, with positive integers d, s . Let $T_n(\mathbf{f})$ be the Toeplitz matrix generated by \mathbf{f} . Then we have*

$$\{T_n(\mathbf{f})\}_n \sim_\sigma \mathbf{f}.$$

Moreover, if \mathbf{f} is a Hermitian matrix-valued function a.e., then

$$\{T_n(\mathbf{f})\}_n \sim_\lambda \mathbf{f}.$$

Concerning the circulant matrix sequences, though the eigenvalues of a circulant matrix $C_n(\mathbf{f})$ are explicitly known, a result like Theorem 1.9 and Theorem 1.10 does not hold for sequences $\{C_n(\mathbf{f})\}_n$ in general. Indeed, the Fourier sum of \mathbf{f} converges to \mathbf{f} under quite restrictive assumptions (see [35]). In particular, if \mathbf{f} belongs to the Dini-Lipschitz class, then $\{C_n(\mathbf{f})\}_n \sim_\lambda \mathbf{f}$, (see [22] for more relationships between circulant sequences and spectral distribution results).

1.4. Matrix algebras. Apart from the circulant algebra introduced in Section 1.2, we recall that other particular matrix algebras have interesting properties and can be exploited for our purpose. In particular, we mention the well-known τ -algebras; see [8] and the references therein. Here, we restrict the analysis to the case of the matrix algebras $\tau_{\varepsilon, \varphi}$ introduced in [8],

where an element of the algebra is a matrix

$$T_{n,\varepsilon,\varphi}(g) = \begin{bmatrix} a + \varepsilon b & b & & & \\ b & a & b & & \\ & \ddots & \ddots & \ddots & \\ & & b & a & b \\ & & & b & a + \varphi b \end{bmatrix}.$$

We can associate to this matrix a function g of the form $g(\theta) = a + 2b \cos \theta$. For some values of ε and φ , the exact eigenvalues of $T_{n,\varepsilon,\varphi}(g)$ are given by a sampling with specific grids; for detailed examples see [7] and [21] for asymptotic results.

In Table 1.2 we provide the proper grids $\theta_{j,n}^{(\varepsilon,\varphi)}$ and $\Theta_{i,j,n}^{(\varepsilon,\varphi)}$ to give the exact eigenvalues and eigenvectors, respectively, for $\varepsilon, \varphi \in \{-1, 0, 1\}$.

TABLE 1.2
Grids for $\tau_{\varepsilon,\varphi}$ -algebras, $\varepsilon, \varphi \in \{-1, 0, 1\}$; $\theta_{j,n}^{(\varepsilon,\varphi)}$ and $\Theta_{i,j,n}^{(\varepsilon,\varphi)}$ are the grids used to compute the eigenvalues and eigenvectors, respectively. For the standard naming convention (dst-) and (dct-*) between parentheses, see, e.g., [14, Appendix 1].*

$\varepsilon \backslash \varphi$		$\theta_{j,n}^{(\varepsilon,\varphi)}$			$\Theta_{i,j,n}^{(\varepsilon,\varphi)}$
		-1	0	1	-1, 0, 1
-1		^(dst-2) $\frac{j\pi}{n}$	^(dst-6) $\frac{j\pi}{n+1/2}$	^(dst-4) $\frac{(j-1/2)\pi}{n}$	$(i-1/2)\theta_{j,n}^{(\varepsilon,\varphi)}$
0		^(dst-5) $\frac{j\pi}{n+1/2}$	^(dst-1) $\frac{j\pi}{n+1}$	^(dst-7) $\frac{(j-1/2)\pi}{n+1/2}$	$i\theta_{j,n}^{(\varepsilon,\varphi)}$
1		^(dct-4) $\frac{(j-1/2)\pi}{n}$	^(dct-8) $\frac{(j-1/2)\pi}{n+1/2}$	^(dct-2) $\frac{(j-1)\pi}{n}$	$(i-1/2)\theta_{j,n}^{(\varepsilon,\varphi)} + \frac{\pi}{2}$

Since all grids $\theta_{j,n}^{(\varepsilon,\varphi)}$ associated with $\tau_{\varepsilon,\varphi}$ -algebras, where $\varepsilon, \varphi \in \{-1, 0, 1\}$, are uniformly spaced grids, we know that

$$\begin{aligned} \theta_{j,n}^{(1,1)} &< \theta_{j,n}^{(0,1)} = \theta_{j,n}^{(1,0)} \\ &< \theta_{j,n}^{(-1,1)} = \theta_{j,n}^{(1,-1)} \\ &< \theta_{j,n}^{(-1,0)} = \theta_{j,n}^{(0,-1)} \\ &< \theta_{j,n}^{(-1,-1)}, \quad \forall j = 1, \dots, n. \end{aligned}$$

For $j = 1, \dots, \lceil n/2 \rceil$,

$$\theta_{j,n}^{(-1,1)} = \theta_{j,n}^{(1,-1)} \leq \theta_{j,n}^{(0,0)},$$

with equality only for $j = \lceil n/2 \rceil$ and n odd.

For $j = \lceil n/2 \rceil + 1, \dots, n$,

$$\theta_{j,n}^{(0,0)} < \theta_{j,n}^{(-1,1)} = \theta_{j,n}^{(1,-1)}.$$

In addition, we observe the further relationship $\theta_{j,n}^{(1,0)} < \theta_{j,n}^{(0,0)}$ for any j , which will be used in equation (2.7).

1.5. Theory of Generalized Locally Toeplitz (GLT) sequences. In this section we introduce the main properties from the theory of Generalized Locally Toeplitz (GLT) sequences and the practical features that are sufficient for our purposes; see [4, 3, 23, 24].

In particular, we consider the multilevel and block setting with d being the number of levels.

GLT1 Each GLT sequence has a singular value symbol $\mathbf{f}(\boldsymbol{\theta}, \mathbf{x})$, which is measurable according to the Lebesgue measure and according to the second item in Definition 1.7 with $\ell = 2d$. In addition, if the sequence is Hermitian, then the distribution also holds in the eigenvalue sense.

We specify that a GLT sequence $\{A_n\}_n$ has GLT symbol $\mathbf{f}(\boldsymbol{\theta}, \mathbf{x})$ by the notation $\{A_n\}_n \sim_{\text{GLT}} \mathbf{f}(\boldsymbol{\theta}, \mathbf{x}), (\boldsymbol{\theta}, \mathbf{x}) \in [-\pi, \pi]^d \times [0, 1]^d$.

GLT2 The set of GLT sequences forms a $*$ -algebra, i.e., it is closed under linear combinations, products, inversion (whenever the symbol is singular on, at most, a set of zero Lebesgue measure), and conjugation. Hence, we obtain the GLT symbol of algebraic operations of a finite set of GLT sequences by performing the same algebraic manipulations of the symbols of the considered GLT sequences.

GLT3 Every Toeplitz sequence $\{T_n(\mathbf{f})\}_n$ generated by a function $\mathbf{f}(\boldsymbol{\theta})$ belonging to the space $L^1([-\pi, \pi]^d)$ is a GLT sequence and with GLT symbol given by \mathbf{f} . Every diagonal sampling sequence $\{D_n(\mathbf{a})\}_n$ generated by a Riemann integrable function $\mathbf{a}(\mathbf{x})$, $\mathbf{x} \in [0, 1]^d$ is a GLT sequence and with GLT symbol given by \mathbf{a} .

GLT4 Every sequence which is distributed as the constant zero in the singular value sense is a GLT sequence with symbol 0. In particular this applies to

- every sequence in which the rank divided by the size tends to zero as the matrix size tends to infinity;
- every sequence in which the trace-norm (i.e., the sum of the singular values) divided by the size tends to zero as the matrix size tends to infinity.

From a practical viewpoint, on the one hand, for a sequence belonging to the GLT class, one of the main advantages is that under certain assumptions, crucial spectral and singular value information can be derived using the concept of the GLT symbol. On the other hand, the above properties imply the following important features of the GLT symbol. Given a sequence $\{A_n\}_n$ obtained by algebraic operations of a finite set of GLT sequences, the small-norm and low-rank terms of which the sequence is composed should be neglected in the computation of the GLT symbol. Consequently, it happens that for small matrix sizes n , the approximations may not be as accurate as desired.

For this reason, in [7], it has been introduced and exploited the concept of (singular value and spectral) “momentary symbols”, starting from the special case of Toeplitz structures. Here we generalize the notion to that of “GLT momentary symbols”: the construction stems from that of the symbol in the GLT sense, but in practice the information of the small-norm contributions is kept in the symbol, and this may lead to higher accuracy, at least in some emblematic cases, when approximating the singular values and eigenvalues of Toeplitz-like matrices, even for small dimensions.

1.6. The GLT momentary symbol sequence. For clarity, in this section we consider the matrix sequences in detail only in the unilevel and scalar setting. We want to avoid a cumbersome notation, but the ideas are extensible in a straightforward manner to the case where the involved GLT symbols are also matrix-valued and multivariate, as briefly sketched.

$$H_n = T_n(i \sin \theta) = \frac{1}{2} \begin{bmatrix} 0 & 1 & & & \\ -1 & 0 & 1 & & \\ & \ddots & \ddots & \ddots & \\ & & -1 & 0 & 1 \\ & & & -1 & 0 \end{bmatrix},$$

which are of importance since $A_n = D_n(a)K_n + E_n$ and $B_n = hD_n(b)H_n$ with $\{E_n\}_n \sim_\sigma 0$, as an immediate check in [5] can show. Therefore, by using the GLT axioms (as done in detail in [5]), we obtain

$$\{A_n\}_n \sim_{\text{GLT}} a(x)(2 - 2 \cos \theta), \quad \left\{ \frac{1}{h} B_n \right\}_n \sim_{\text{GLT}} ib(x) \sin \theta, \quad \left\{ \frac{1}{h^2} C_n \right\}_n \sim_{\text{GLT}} c(x).$$

As a conclusion $\{B_n\}_n \sim_{\text{GLT}} 0$, $\{C_n\}_n \sim_{\text{GLT}} 0$, and hence, setting $X_n = A_n + B_n + C_n$ the actual coefficient matrix of the linear system in (1.6), again by the $*$ -algebra structure of the GLT matrix sequences, we deduce

$$\{X_n\}_n \sim_{\text{GLT}} a(x)(2 - 2 \cos \theta).$$

Now, following [7], the idea is to consider not only the asymptotic setting but also the case of moderate sizes. As a consequence, for increasing the precision of the evaluation of eigenvalues and singular values, we can associate to

$$X_n = A_n + B_n + C_n$$

the specific symbol $f_n(x, \theta) = a(x)(2 - 2 \cos \theta) + hib(x) \sin \theta + h^2 c(x)$.

We are now in position to give a formal definition of GLT momentary symbols.

DEFINITION 1.11 (GLT momentary symbols). *Let $\{X_n\}_n$ be a matrix sequence, and assume that there exist matrix sequences $\{A_n^{(j)}\}_n$, $\{R_n\}_n$, scalar sequences $c_n^{(j)}$, $j = 0, \dots, t$, and measurable functions f_j defined over $[-\pi, \pi] \times [0, 1]$, and with t a nonnegative integer independent of n , such that $\{R_n\}_n$ is zero-distributed (as in item **GLT4** in Section 1.5),*

$$(1.7) \quad \begin{aligned} & \left\{ \frac{A_n^{(j)}}{c_n^{(j)}} \right\}_n \sim_{\text{GLT}} f_j, \\ & c_n^{(0)} = 1, \quad c_n^{(s)} = o(c_n^{(r)}), \quad t \geq s > r, \\ & \{X_n\}_n = \{A_n^{(0)}\}_n + R_n + \sum_{j=1}^t \{A_n^{(j)}\}_n. \end{aligned}$$

Then, with a slight abuse of notation,

$$(1.8) \quad f_n = f_0 + \sum_{j=1}^t c_n^{(j)} f_j$$

is defined as the GLT momentary symbol for X_n , and $\{f_n\}$ is the sequence of GLT momentary symbols for the matrix sequence $\{X_n\}_n$.

Of course, in line with Section 1.5, the momentary symbol could be matrix-valued with a number of variables equal to $2d$ and domain $[-\pi, \pi]^d \times [0, 1]^d$ if the basic matrix sequences

appearing in Definition 1.11 are, up to proper scaling, matrix-valued and multilevel GLT matrix sequences. For example in the scalar d -variate setting, relation (1.8) takes the form

$$f_n = \sum_{j=0}^t c_n^{(j)} f_j,$$

which is a plain multivariate (possibly block) version of (1.8).

Clearly there is a link with GLT theory stated in the next result.

THEOREM 1.12. *Assume that the matrix sequence $\{X_n\}_n$ satisfies the requirements in Definition 1.11. Then, $\{X_n\}_n$ is a GLT matrix sequence, and the GLT symbol f_0 of the main term $A_n^{(0)}$ is the GLT symbol of $\{X_n\}_n$, that is, $\{X_n\}_n \sim_{\text{GLT}} f_0$ and $\lim_{n \rightarrow \infty} f_n = f_0$ a.e. on the definition domain.*

Proof. Since f_n is a linear combination of measurable functions, f_n is still a measurable function. Furthermore, because $c_n^{(j)} \rightarrow 0$ as $n \rightarrow \infty$, for all $j = 1, \dots, t$, we deduce that for all $\epsilon > 0$

$$\lim_{n \rightarrow \infty} m \{x \in D : |f_n - f_0| > \epsilon\} = 0,$$

and therefore f_n converges a.e. to f_0 as n tends to infinity.

From the point of view of the considered matrix sequences, the relation

$$\left\{ \frac{A_n^{(j)}}{c_n^{(j)}} \right\}_n \sim_{\text{GLT}} f_j,$$

with $c_n^{(j)}$ infinitesimal for all $j = 1, \dots, t$, implies $\left\{ A_n^{(j)} \right\}_n \sim_{\text{GLT}, \sigma} 0$ for all $j = 1, \dots, t$, while we know that $\{R_n\}_n \sim_{\text{GLT}, \sigma} 0$ by the assumption and item **GLT4**. From the $*$ -algebra structure of the GLT matrix sequences, we infer that

$$\{X_n\}_n \sim_{\text{GLT}} f_0,$$

and hence the proof is concluded. \square

The given definition of momentary symbols is inspired, as it is clear from the initial example of a diffusion-convection-advection equation, by the example of approximated differential equations, where the presence of differential operators of different orders induces, after a possible proper scaling, a structure like that reported in (1.7).

The idea is that the momentary symbol can be used for giving a more precise evaluation either of the spectrum or of the eigenvalues for moderate sizes of the matrices and not only asymptotically. However, we should be aware that, intrinsically, there is no general recipe especially for the eigenvalues. In fact, as already proven in [30], a rank-one perturbation of infinitesimal spectral norm actually can change the spectra of matrix sequences, sharing the same GLT symbol and even sharing the same sequence of momentary symbols.

EXAMPLE 1. Take the matrices $T_n(e^{i\theta})$, and let $X_n = T_n(e^{i\theta}) + e_1 e_n^T c_n^{(1)}$ with $c_n^{(1)} = n^{-\alpha}$ and $\alpha > 0$ any positive number independent of the matrix size n . By direct inspection $\{e_1 e_n^T c_n^{(1)}\}_n \sim_{\sigma} 0$, and hence it is a GLT matrix sequence with zero symbol, independently of the parameter α . If we look at the GLT momentary symbols, then they coincide with the GLT symbol for both $\{T_n(e^{i\theta})\}_n$ and $\{X_n\}_n$. However, while in the first case the eigenvalues are all equal to zero, in the second case they distribute asymptotically as the GLT symbol $e^{i\theta}$ (which is also the GLT momentary symbol for any n).

EXAMPLE 2. Take a positive function a defined on $[0, 1]$, the matrices $D_n(a)T_n(e^{i\theta})$, and $X_n = D_n(a)T_n(e^{i\theta}) + e_1 e_n^T c_n^{(1)}$ with $c_n^{(1)} = n^{-\alpha}$ and $\alpha > 0$ any positive number independent of the matrix size n . Since $\{e_1 e_n^T c_n^{(1)}\}_n$ is a GLT matrix sequence with zero symbol independent of the parameter α , we deduce that both $\{D_n(a)T_n(e^{i\theta})\}_n$ and $\{X_n\}_n$ share the same GLT symbol $a(x)e^{i\theta}$ (which is also the momentary symbol for any n). Again there is a dramatic change: while in the first case the eigenvalues are all equal to zero, in the second case they distribute asymptotically as the function $\hat{a}e^{i\theta}$, where \hat{a} is the limit (if it exists) of the geometric mean of sampling values present in $D_n(a)$ as n tends to infinity. Since $n^{-\alpha/n}$ converges to 1 independently of the parameter α as n tends to infinity, \hat{a} will depend only on the diagonal values of $D_n(a)$. As a conclusion, the eigenvalue distributions do not coincide with the GLT momentary symbols, and this is a message that the present tool could be ineffective and even misleading, when very non-normal matrices are considered.

In this setting it must be emphasized that the asymptotic eigenvalue distribution is discontinuous with respect to the standard norms or metrics widely considered in the context of matrix sequences.

As a conclusion of the present section, we report preliminary numerical evidence of the use of GLT momentary symbols for having a more precise estimate of the spectrum when compared with the standard GLT symbol, at least for moderate matrix orders. Consider the coefficient matrices in (1.6) approximating the linear differential operator in (1.5). For the sake of simplicity we consider $b(x) \equiv 0$ so that the related matrices are real symmetric positive definite. As first case we take $a(x) = 1 + x^2$ and $c(x) = 6 + \sin(x^3)$. We compute E_s and E_{ms} , which are the averaged sum of the absolute errors, using as reference functions the GLT symbol

$$f_s(x, \theta) = a(x)(2 - 2 \cos \theta)$$

and the associated GLT momentary symbols

$$f_{ms}(x, \theta) = a(x)(2 - 2 \cos \theta) + h^2 c(x),$$

respectively. In both cases, we pick $n = \nu^2$, and we sample with

$$x_i = i/(\nu + 1), \quad i = 1, \dots, \nu, \quad \theta_j = j\pi/(\nu + 1), \quad j = 1, \dots, \nu$$

by rearranging in non-decreasing order in order to compare with the true eigenvalues.

As already mentioned, E_s is the averaged sum of the absolute errors when comparing sorted eigenvalues with sorted symbol approximations with the grid given above. E_{ms} is analogously defined but for the related GLT momentary symbols.

We observe that the estimates provided by the GLT momentary symbols are always better with this metric, and in addition we have $E_s - E_{ms} > 0$, which is not theoretically expected. Indeed Table 1.3 shows the advantage for moderate matrix sizes, while the advantage becomes less evident when the matrix sizes grow.

We tested several other examples, and we observed an advantage for moderate sizes, while this is not necessarily true for matrices of large order and it depends on the sampling grid.

2. All-at-once solution of parabolic problems. The aim of this section is that of describing as accurately as possible the spectra and singular values of the structured linear system sequence stemming from the space-time discretization of a parabolic diffusion problem. Thus, we consider the diffusion equation in one space dimension,

$$u_t = u_{xx}, \quad x \in (a, b), \quad t \in [0, T],$$

TABLE 1.3
 Comparison between the averaged sum of the errors with $a(x) = 1 + x^2$ and $c(x) = 6 + \sin(x^3)$.

n	E_s $n^{-1} \sum \lambda_j - f_s(x, \theta) $	E_{ms} $n^{-1} \sum \lambda_j - f_{ms}(x, \theta) $	$E_s - E_{ms}$
9	0.31659454914897317	0.29510847614861735	$2.148607300035582 \cdot 10^{-2}$
16	0.22558459755745924	0.2198017354258519	$5.782862131607336 \cdot 10^{-3}$
25	0.18608391764879742	0.18492972171356425	$1.1541959352331654 \cdot 10^{-3}$
36	0.16554176225430134	0.1655179810161299	$2.378123817142752 \cdot 10^{-5}$
49	0.14997522607499242	0.14991040173853432	$6.482433645810248 \cdot 10^{-5}$
64	0.1316103011775121	0.13148627818739497	$1.2402299011712858 \cdot 10^{-4}$
81	0.11825980438015823	0.11822102653019283	$3.877784996540734 \cdot 10^{-5}$
100	0.10762803505912259	0.1076237122985601	$4.322760562489036 \cdot 10^{-6}$
400	0.057367307847965725	0.05736596577310507	$1.3420748606537969 \cdot 10^{-6}$
900	0.03901486832603214	0.03901462915216716	$2.391738649770714 \cdot 10^{-7}$
1600	0.029525883049866225	0.029525795496153927	$8.75537122975445 \cdot 10^{-8}$

where we prescribe u at $t = 0$ and impose a periodicity condition $u(x \pm (b - a), t) = u(x, t)$.

We approximate our parabolic model problem on a rectangular space-time grid consisting of N_t time intervals and N_x space intervals. We obtain a sequence of linear systems in which each component is of the form

$$(2.1) \quad A_{\mathbf{n}}x = b, \quad A_{\mathbf{n}} = J_{N_t} \oplus Q_{N_x} = J_{N_t} \otimes \mathbb{I}_{N_x} + \mathbb{I}_{N_t} \otimes Q_{N_x} \in \mathbb{R}^{N \times N}, \quad x, b \in \mathbb{R}^N,$$

where $N = N_t N_x$, $\mathbf{n} = (N_t, N_x)$, \mathbb{I}_m is the identity matrix of size m , and the matrices J_{N_t} and Q_{N_x} come from the discretizations in time and space, respectively. In the following, we describe the time and space discretization and, in particular, how this leads to structured components of the matrix $A_{\mathbf{n}}$.

2.1. Time discretization. The principal ingredients of the time discretization are:

- Choosing N_t equispaced points in $[0, T]$ with stepsize $h_t = T/N_t$, that is, $t_j = jh_t$, for $j = 1, \dots, N_t$.
- A discretization in time by a standard backwards Euler scheme.

Regarding notations, for the sake of simplicity, since we are considering a 2D problem, the symbols will have as Fourier variable (θ, ξ) instead of the standard choice (θ_1, θ_2) indicated in the notations of Section 1.2 (see Definition 1.4).

The resulting matrix is J_{N_t} , which has the following unilevel scalar Toeplitz structure:

$$(2.2) \quad J_{N_t} = \frac{1}{h_t} \begin{bmatrix} 1 & & & & \\ -1 & 1 & & & \\ & \ddots & \ddots & & \\ & & & -1 & 1 \end{bmatrix} = \frac{1}{h_t} T_{N_t}(f_J),$$

where f_J is the generating function of the matrix sequence $\{T_n(f_J)\}_n$ with

$$f_J(\theta) = 1 - e^{i\theta}.$$

2.2. Space discretization. The principal elements of the space discretization are:

- Choosing N_x equispaced points in $[a, b]$. Since we are considering periodic boundary conditions, we have as step size $h_x = (a - b)/N_x$ and $x_j = h_x(j - 1)$, for $j = 1, \dots, N_x$.
- A discretization in space using second-order finite differences.

Consequently, the space discretization matrix will be the circulant matrix Q_{N_x} of the form:

$$Q_{N_x} = \frac{1}{h_x^2} \begin{bmatrix} 2 & -1 & & & -1 \\ -1 & 2 & -1 & & \\ & \ddots & \ddots & \ddots & \\ & & -1 & 2 & -1 \\ -1 & & & -1 & 2 \end{bmatrix} = \frac{1}{h_x^2} C_{N_x}(f_Q),$$

where

$$f_Q(\xi) = 2 - 2 \cos \xi$$

is the generating function of the matrix.

Of course a choice of Dirichlet boundary conditions would lead to the standard discrete Laplacian $T_{N_x}(f_Q)$: the analysis is equivalent since also this matrix admits a well-known diagonalization matrix that is the sine transform matrix of type I, which is real, orthogonal, and symmetric.

2.3. Analysis of the coefficient matrix A_n . We have seen that discretizing the problem of interest for a sequence of discretization parameters h_x and h_t leads to a sequence of linear systems whose approximation error tends to zero as the coefficient matrix size grows to infinity. The n th coefficient matrix component is of the form

$$(2.3) \quad A_n = \frac{1}{h_t} T_{N_t}(f_J) \otimes \mathbb{I}_{N_x} + \mathbb{I}_{N_t} \otimes \frac{1}{h_x^2} C_{N_x}(f_Q).$$

In order to design efficient solvers for the considered linear systems, it is of crucial importance to know the spectral properties of the matrix sequence $\{A_n\}_n$. Hence, this section is devoted to the analysis of the structure of the matrix sequence $\{A_n\}_n$ in (2.1). In particular, we provide the singular values and spectral analysis using algebraic tricks, GLT theory, and the concept of GLT momentary symbols.

2.4. GLT analysis of the coefficient sequence $\{A_n\}_n$. The asymptotic spectral and singular value distributions for the matrix size $d(n)$ sufficiently large of the matrix sequence $\{A_n\}_n$ depend on how h_x and h_t approach zero. Letting $c_h := h_x^2/h_t$, we have three different cases to consider.

CASE 1. $[c_h \rightarrow \infty]$: If $h_t \rightarrow 0$ faster than $C_1 h_x^2$, where C_1 is a constant, then we can consider the matrix

$$h_t A_n = T_{N_t}(f_J) \otimes \mathbb{I}_{N_x} + \mathbb{I}_{N_t} \otimes \underbrace{\frac{h_t}{h_x^2}}_{c_h^{-1} \rightarrow 0} C_{N_x}(f_Q).$$

Then, the sequence satisfies $\{h_t A_n\}_n = \{T_{N_t}(f_J) \otimes \mathbb{I}_{N_x} + \mathbb{N}_n\}_n$, where \mathbb{N}_n is a small-norm matrix in the sense of item 2 of property **GLT4** with $\|\mathbb{N}_n\| < C_2$, C_2 constant. Consequently, from **GLT4**, $\{\mathbb{N}_n\}_n$ is a matrix sequence distributed in the singular value sense as 0, which implies that $\{\mathbb{N}_n\}_n$ is zero-distributed in the GLT sense as described in **GLT4**. Moreover, since f_J is a trigonometric polynomial, Theorem 1.10, properties **GLT1–GLT4**, and Lemma 1.6 imply that

$$\{h_t A_n\}_n \sim_{\text{GLT}} f_J(\theta) \otimes 1 + 1 \otimes 0 = f_A^{(1)}(\theta, \xi).$$

The 1 present in $f_J(\theta) \otimes 1$ should be interpreted as $1e^{0i\xi}$, and $1 \otimes 0$ should be interpreted as $1e^{0i\theta} \otimes 0e^{0i\xi}$. Hence, the GLT symbol of the sequence $\{h_t A_n\}_n$ is the bivariate function

$$f_A^{(1)}(\theta, \xi) = f_J(\theta) = 1 - e^{i\theta},$$

and it should be interpreted as the function $f_J(\theta) \otimes 1$, which is constant in the second component.

From the property **GLT1**, the function $f_A^{(1)}(\theta, \xi)$ describes the singular value distribution in the sense of relation (1.3). In more detail,

$$\{h_t A_n\}_n \sim_{\text{GLT}, \sigma} 1 - e^{i\theta}.$$

However, the matrix sequence $\{h_t A_n\}_n$ is not symmetric, hence the distribution may not hold in the eigenvalue sense (see also Example 1 and Example 2 at the end of Section 1.6), and in this specific case actually it does not hold with the function $1 - e^{i\theta}$: in fact, if a real symmetric (or Hermitian) matrix sequence has an eigenvalue distribution function, then this function is necessarily real-valued almost everywhere; conversely, a non-Hermitian matrix sequence can have a real-valued eigenvalue distribution function (there are indeed many possible concrete examples). Because of the structure of $J_{N_t} = \frac{1}{h_t} T_{N_t}(f_J)$ in equation (2.2), it is straightforward to see that the asymptotic spectral distribution is given by $\mathfrak{f}(\theta, \xi) = 1$, according to relation (1.4), that is,

$$\{h_t A_n\}_n \sim_{\lambda} 1.$$

CASE 2. $[c_h \rightarrow 0]$: If $h_x^2 \rightarrow 0$ faster than $C_1 h_t$, where C_1 is a constant, then we have

$$h_x^2 A_n = \underbrace{\frac{h_x^2}{h_t}}_{c_h \rightarrow 0} T_{N_t}(f_J) \otimes \mathbb{I}_{N_x} + \mathbb{I}_{N_t} \otimes C_{N_x}(f_Q).$$

Then, the sequence satisfies $\{h_x^2 A_n\}_n = \{\mathbb{N}_n + \mathbb{I}_{N_t} \otimes C_{N_x}(f_Q)\}_n$, where \mathbb{N}_n is a small-norm matrix in the sense of item 2 of property **GLT4** with $\|\mathbb{N}_n\| < C_2$, C_2 constant. Hence, $\{\mathbb{N}_n\}_n$ is a matrix sequence distributed in the singular value sense, and consequently in the GLT sense, as 0. Moreover, f_Q belongs to the Dini-Lipschitz class, consequently, properties **GLT2–GLT4** and Lemma 1.6 imply that

$$\{h_x^2 A_n\}_n \sim_{\text{GLT}} 0 \otimes 1 + 1 \otimes f_Q(\xi) = 1 \otimes f_Q(\xi) = f_A^{(2)}(\theta, \xi),$$

where the GLT symbol is given by

$$f_A^{(2)}(\theta, \xi) = f_Q(\xi) = 2 - 2 \cos \xi.$$

In this case the function $f_A^{(2)}(\theta, \xi)$ is a singular value symbol for the sequence $\{h_x^2 A_n\}_n$ and also an eigenvalue symbol since the matrices $C_{N_x}(f_Q)$ are Hermitian for each N_x . Hence we have

$$\{h_x^2 A_n\}_n \sim_{\text{GLT}, \sigma, \lambda} 2 - 2 \cos \xi.$$

CASE 3. $[c_h = c = \text{constant}]$: The last case is when h_x^2 and h_t are proportional and related by the constant $c_h = c = \frac{h_x^2}{h_t}$ independent of the various step-sizes. In this setting we

have

$$h_x^2 A_n = \underbrace{\frac{h_x^2}{h_t}}_{c_h} T_{N_t}(f_J) \otimes \mathbb{I}_{N_x} + \mathbb{I}_{N_t} \otimes C_{N_x}(f_Q).$$

Consequently, from **GLT2**, **GLT3**, and Lemma 1.6, the following relationship holds when c_h is a constant

$$\{h_x^2 A_n\}_n \sim_{\text{GLT}} c f_J(\theta) \otimes 1 + 1 \otimes f_Q(\xi) = f_A^{(3)}(\theta, \xi).$$

From considerations analogous to the case 1 and 2, we have

$$\{h_x^2 A_n\}_n \sim_{\text{GLT}, \sigma} c(1 - e^{i\theta}) + (2 - 2 \cos \xi).$$

Since the matrix $h_x^2 A_n$ is not Hermitian, the eigenvalue symbol $f(\theta, \xi)$ cannot be directly derived by $f_A^{(3)}(\theta, \xi)$ (see again the discussion in the examples after Definition 1.11).

In this setting the situation is simple because the involved two-level structure can be simply block-diagonalized, while the use of the GLT momentary symbol becomes useful in approximating the singular values of the sequence $\{h_x^2 A_n\}_n$.

2.5. Analysis of the coefficient matrix sequence $\{A_n\}_n$ by algebraic manipulations and GLT momentary symbols. The first observation is that the matrix in (2.3) admits a decomposition which shows in evidence a lower-triangular matrix, which is similar to the original one, and hence all the eigenvalues are known exactly. In fact, by looking carefully at (2.3), we obtain that

$$\frac{1}{h_t} T_{N_t}(f_J) \otimes \mathbb{I}_{N_x} = \mathbb{I}_{N_t} \left[\frac{1}{h_t} T_{N_t}(f_J) \right] \mathbb{I}_{N_t} \otimes \mathbb{F}_{N_x} \mathbb{I}_{N_x} \mathbb{F}_{N_x}^*$$

and

$$\mathbb{I}_{N_t} \otimes \frac{1}{h_x^2} C_{N_x}(f_Q) = \mathbb{I}_{N_t} \mathbb{I}_{N_t} \mathbb{I}_{N_t} \otimes \mathbb{F}_{N_x} \frac{1}{h_x^2} D_{N_x} \mathbb{F}_{N_x}^*,$$

where \mathbb{F}_{N_x} is the unitary Fourier matrix of size N_x , $\mathbb{F}_{N_x}^*$ is its transpose conjugate and hence its inverse, and D_{N_x} is the diagonal matrix containing the eigenvalues of $C_{N_x}(f_Q)$, that is, $f_Q(2\pi j/N_x) = 2 - 2 \cos(2\pi j/N_x)$, $j = 0, 1, \dots, N_x - 1$.

Since $T_{N_t}(f_J)$ is a lower bidiagonal matrix with 1 on the main diagonal, it can be easily seen that the eigenvalues of A_n in (2.3) are exactly

$$\frac{1}{h_t} + \frac{1}{h_x^2} (2 - 2 \cos(2\pi j/N_x)), \quad j = 0, 1, \dots, N_x - 1,$$

each of them with multiplicity N_t . As a consequence, by taking a proper normalization, the spectral radius $\rho(h_x^2 A_n)$ will coincide simply with $4 + c_h$.

It is clear that in this context, due to the high non-normality of the term $T_{N_t}(f_J)$, after proper scalings depending on h_t and h_x , the eigenvalues are a uniform sampling of the function

$$\frac{h_t}{h_x^2} (2 - 2 \cos \theta),$$

which is not the GLT symbol and is not the associated GLT momentary symbol. The latter statement is not surprising given the discussion regarding the asymptotic behaviour of the

matrix sequences reported in Example 1 and in Example 2, when discussing the potential and the limitations of the notion of GLT momentary symbols. Also in this setting, by imposing (quite artificial) periodic boundary conditions in time, the term $T_{N_t}(f_J)$ will change into $C_{N_t}(f_J)$, and magically a one-rank correction repeated N_t times to the matrix A_n will produce a new matrix with the same GLT and momentary symbols as before: however, in this case the eigenvalues will be exactly the sampling of such functions. This is a further confirmation of the delicacy of the eigenvalues, which can have dramatic changes due to minimal corrections, when we are in a context of highly non-normal matrices.

2.5.1. Singular values of $h_x^2 A_n$ (exact). The singular values $\sigma_1(h_x^2 A_n), \dots, \sigma_{d(\mathbf{n})}(h_x^2 A_n)$ of the matrix $h_x^2 A_n$ are given by the positive square roots of the eigenvalues of the Hermitian matrix $h_x^4 A_n A_n^T$. Hence, in order to provide exactly $\sigma_i(h_x^2 A_n)$, $i = 1, \dots, d(\mathbf{n})$, we are interested in the spectrum of the matrix

$$h_x^4 A_n A_n^T = \begin{bmatrix} \tilde{Q}_{N_x}^2 & -c_h \tilde{Q}_{N_x} & & & & \\ -c_h \tilde{Q}_{N_x} & \tilde{Q}_{N_x}^2 + c_h^2 \mathbb{I}_{N_x} & -c_h \tilde{Q}_{N_x} & & & \\ & -c_h \tilde{Q}_{N_x} & \tilde{Q}_{N_x}^2 + c_h^2 \mathbb{I}_{N_x} & \ddots & & \\ & & \ddots & \ddots & & \\ & & & \ddots & \ddots & -c_h \tilde{Q}_{N_x} \\ & & & & -c_h \tilde{Q}_{N_x} & \tilde{Q}_{N_x}^2 + c_h^2 \mathbb{I}_{N_x} \end{bmatrix},$$

where $\tilde{Q}_{N_x} = C_{N_x} + c_h \mathbb{I}_{N_x}$. Note that $h_x^4 A_n A_n^T$ is not a pure block-tridiagonal Toeplitz matrix because of the missing constant c_h^2 in the block in the top left corner. However, for each fixed N_t and N_x , the matrix \tilde{Q}_{N_x} is a circulant matrix with generating function $f_{\tilde{Q}_{N_x}}(\xi) = 2 - 2 \cos \xi + c_h$, which is also its GLT momentary symbol. Thus we infer that $h_x^4 A_n A_n^T$ is similar to a matrix $X_{d(\mathbf{n})}$ whose explicit expression is reported below:

$$h_x^4 A_n A_n^T \sim X_{d(\mathbf{n})} = \begin{bmatrix} D_{\tilde{Q}}^2 & -c_h D_{\tilde{Q}} & & & & \\ -c_h D_{\tilde{Q}} & D_{\tilde{Q}}^2 + c_h^2 \mathbb{I}_{N_x} & -c_h D_{\tilde{Q}} & & & \\ & -c_h D_{\tilde{Q}} & D_{\tilde{Q}}^2 + c_h^2 \mathbb{I}_{N_x} & \ddots & & \\ & & \ddots & \ddots & & \\ & & & \ddots & \ddots & -c_h D_{\tilde{Q}} \\ & & & & -c_h D_{\tilde{Q}} & D_{\tilde{Q}}^2 + c_h^2 \mathbb{I}_{N_x} \end{bmatrix},$$

with $D_{\tilde{Q}} = \text{diag}_{\ell=1, \dots, N_x} (f_{\tilde{Q}_{N_x}}(\xi_{\ell, N_x}))$. Consequently we study the spectrum of $X_{d(\mathbf{n})}$ to attain formulas for the exact singular values of $h_x^2 A_n$. Let us consider a permutation matrix P that transforms $X_{d(\mathbf{n})}$ into an $N_t \times N_t$ block diagonal matrix $P X_{d(\mathbf{n})} P^T$, which has on the main diagonal, for $k = 1, \dots, N_x$, blocks of the form

$$(2.4) \quad (P X_{d(\mathbf{n})} P^T)_{i,j=(k-1)N_t+1}^{kN_t} = \begin{bmatrix} C_k^2 & -c_h C_k & & & & \\ -c_h C_k & C_k^2 + c_h^2 & -c_h C_k & & & \\ & -c_h C_k & C_k^2 + c_h^2 & \ddots & & \\ & & \ddots & \ddots & & \\ & & & \ddots & \ddots & -c_h C_k \\ & & & & -c_h C_k & C_k^2 + c_h^2 \end{bmatrix},$$

where $C_k = D_{\tilde{Q}}(k, k) = f_{\tilde{Q}_{N_x}}(\xi_{k, N_x})$.

Hence, the union of the eigenvalues of all blocks of $PX_{d(\mathbf{n})}P^T$ is equivalent to the full spectrum of $h_x^4 A_{\mathbf{n}} A_{\mathbf{n}}^T$. These local eigenvalue problems can be solved analytically (or numerically) independently of each other. For example for $N_t = 2$, we have for every $k = 1, \dots, N_x$ the characteristic equation

$$\begin{vmatrix} \left(f_{\tilde{Q}_{N_x}}(\xi_{k, N_x})\right)^2 - \lambda & -c_h(f_{\tilde{Q}_{N_x}}(\xi_{k, N_x})) \\ -c_h(f_{\tilde{Q}_{N_x}}(\xi_{k, N_x})) & \left(f_{\tilde{Q}_{N_x}}(\xi_{k, N_x})\right)^2 + c_h^2 - \lambda \end{vmatrix} = 0.$$

Thus, we have as singular values the union, for $k = 1, \dots, N_x$, of the quantities

$$\begin{aligned} \sigma^{(1)}(k, c_h) &= \sqrt{\frac{2(f_{\tilde{Q}_{N_x}}(\xi_{k, N_x}))^2 + c_h^2}{2} - \frac{c_h}{2} \sqrt{4(f_{\tilde{Q}_{N_x}}(\xi_{k, N_x}))^2 + c_h^2}}, \\ \sigma^{(2)}(k, c_h) &= \sqrt{\frac{2(f_{\tilde{Q}_{N_x}}(\xi_{k, N_x}))^2 + c_h^2}{2} + \frac{c_h}{2} \sqrt{4(f_{\tilde{Q}_{N_x}}(\xi_{k, N_x}))^2 + c_h^2}}. \end{aligned}$$

Clearly, solving the characteristic equation for $k = 1, \dots, N_x$ becomes more and more complex as N_t grows. Hence, in the next section we provide two possible approximations given by GLT theory and by the GLT momentary formulations.

2.5.2. Singular values of $h_x^2 A_{\mathbf{n}}$ (approximation) via GLT momentary symbols. For the case 2 in Section 2.4 and in Section 2.5, we have already shown that

$$\{h_x^2 A_{\mathbf{n}}\}_{\mathbf{n}} \sim_{\sigma} f_A^{(2)}(\theta, \xi) = 2 - 2 \cos \xi,$$

and the subsequent sequence $\{f_{\mathbf{n}}^{(2)}\}_{\mathbf{n}}$ with

$$f_{\mathbf{n}}^{(2)}(\theta, \xi) = c_h(1 - e^{i\theta}) + (2 - 2 \cos \xi)$$

is the sequence of GLT momentary functions.

Remark 1.8 suggests to exploit these relations in order to obtain a better approximation of the singular values of $h_x^2 A_{\mathbf{n}}$ with respect to the information obtained by the pure GLT symbol. In the following, we compute the quantities $|f_A^{(2)}(\theta, \xi)|$ and $|f_{\mathbf{n}}^{(2)}(\theta, \xi)|$ using the specific grid

$$(2.5) \quad \theta_{j, N_t} = \frac{j\pi}{N_t + 1}, \quad j = 1, \dots, N_t \quad \xi_{\ell, N_x} = \frac{2\pi(\ell - 1)}{N_x}, \quad \ell = 1, \dots, N_x.$$

We can observe in Figure 2.1 that the singular values of $h_x^2 A_{\mathbf{n}}$ (blue circles) are well approximated by sampling $|f_{\mathbf{n}}^{(2)}(\theta, \xi)|$ on the grid (2.5) (red stars). The approximation by using $|f_A^{(2)}(\theta, \xi)|$ instead is good when c_h is small (see the top panel of Figure 2.1 for $N_t = 2$ and $N_x = 10$), but it tends to become a substantially less accurate approximation otherwise; see the bottom panel of Figure 2.1 and Figure 2.2, where $N_t = 10$ and $N_x = 10$.

2.5.3. The 2-norm of $h_x^2 A_{\mathbf{n}}$ (approximation). In the following we are interested in providing a bound for the 2-norm of the matrix $h_x^2 A_{\mathbf{n}}$. When referring to the singular values of $h_x^2 A_{\mathbf{n}}$, we will not assume the standard ordering

$$\sigma_1(h_x^2 A_{\mathbf{n}}) \geq \sigma_2(h_x^2 A_{\mathbf{n}}) \geq \dots \geq \sigma_{d(\mathbf{n})}(h_x^2 A_{\mathbf{n}})$$

since it is more natural to associate the ordering to the equispaced grid of the domain of the related GLT symbol. By definition we have $\|h_x^2 A_{\mathbf{n}}\|_2 = \max_{j=1, \dots, d(\mathbf{n})} \sigma_j(h_x^2 A_{\mathbf{n}})$.

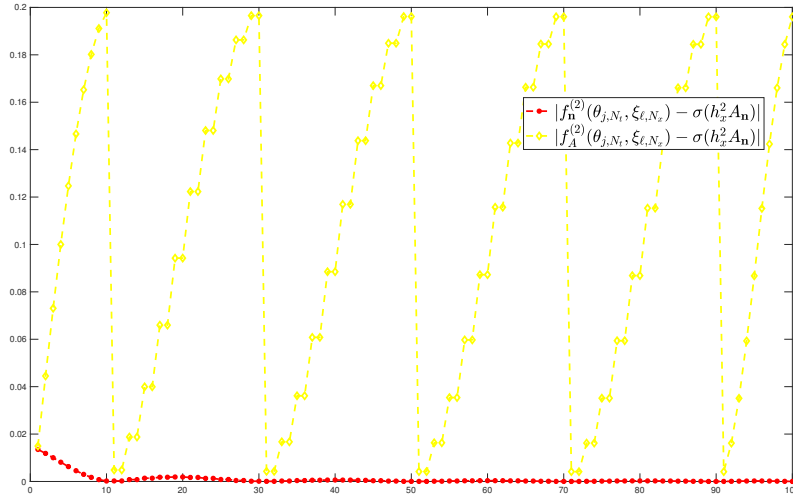


FIG. 2.2. Singular values and samplings of $|f_A^{(2)}(\theta, \xi)|$ and $|f_n^{(2)}(\theta, \xi)|$ for $N_t = 10$ and $N_x = 10$ on the grid in (2.5).

In our case

$$a = (4 + c_h)^2 + c_h^2, \quad b = -c_h(4 + c_h),$$

and the matrix belongs to the $\tau_{\frac{c_h}{4+c_h}, 0}$ -algebra since the element with indices $i, j = 1$ is $a + (c_h/(4 + c_h))b$. Hence, we have $g(\theta) = (4 + c_h)^2 + c_h^2 - 2c_h(4 + c_h)\cos\theta$, which coincides with the momentary symbol \mathfrak{g}_n of the matrix (2.6). Due to the interlacing theorem (see [6, Cor III.1.5]), the irreducible tridiagonal character of $h_x^2 A_n$, and the specific relation between algebras [7], the following relationships can be derived

$$\begin{aligned}
 (2.7) \quad & \underbrace{\mathfrak{g}_n \left(\frac{\pi(N_t - 1/2)}{N_t + 1/2} \right)}_{\max(\lambda_j(T_{N_t, 1, 0}(g)))} < \underbrace{\|h_x^2 A_n\|_2^2}_{\max(\lambda_j(T_{N_t, c_h/(4+c_h), 0}(g)))} \\
 & < \underbrace{\mathfrak{g}_n \left(\frac{\pi N_t}{N_t + 1} \right)}_{\max(\lambda_j(T_{N_t, 0, 0}(g)))} < \underbrace{\mathfrak{g}_n(\pi)}_{\max(\lambda_j(T_{N_t, -1, -1}(f))) = \max(\mathfrak{g}_n)}.
 \end{aligned}$$

As a consequence, good upper and lower bounds for the 2-norm of $h_x^2 A_n$ are reported in the following set of inequalities:

$$\sqrt{\mathfrak{g}_n \left(\frac{\pi(N_t - 1/2)}{N_t + 1/2} \right)} < \|h_x^2 A_n\|_2 < \sqrt{\mathfrak{g}_n \left(\frac{\pi N_t}{N_t + 1} \right)}.$$

In Table 2.1 we present approximations of the 2-norm of $h_x^2 A_n$ using the grid sampling from $\tau_{1,0}$ (lower bound), $\tau_{0,0}$ (upper bound), and $\tau_{-1,-1}$. Note that the sampling on the latter grid is equivalent to a sampling of the singular value momentary symbols $f_n^{(2)}(\theta, \xi)$ at their maximum point. The two-norm $\|h_x^2 A_n\|_2$ is computed numerically. We see that the 2-norm

is well described by the two bounds given above, as N_t increases. Hence, for this type of example, the GLT momentary symbols provide, at least for moderate sizes, a more precise alternative to the pure GLT symbol.

TABLE 2.1
Approximations of the 2-norm for different N_t and c_h . The upper and lower bounds have as their maximum $\sqrt{\max \mathfrak{g}_n} = 4 + 2c_h$.

N_t	c_h	$\sqrt{\mathfrak{g}_n \left(\frac{\pi(N_t-1/2)}{N_t+1/2} \right)}$	$\ h_x^2 A_n\ _2$	$\sqrt{\mathfrak{g}_n \left(\frac{\pi N_t}{N_t+1} \right)}$	$4 + 2c_h$
1	1/8	4.06394205	4.12500000	4.12689350	4.25
10	1/8	4.24460651	4.24505679	4.24508270	4.25
100	1/8	4.24994073	4.24994128	4.24994131	4.25
1000	1/8	4.24999940	4.24999940	4.24999940	4.25
<hr/>					
1	1	4.58257569	5.00000000	5.09901951	6.00
10	1	5.96286240	5.96511172	5.96614865	6.00
100	1	5.99959287	5.99959555	5.99959689	6.00
1000	1	5.99999589	5.99999589	5.99999590	6.00
<hr/>					
1	8	10.58300524	12.00000000	14.42220510	20.00
10	8	19.78560029	19.78964627	19.80461186	20.00
100	8	19.99765486	19.99765952	19.99767802	20.00
1000	8	19.99997634	19.99997634	19.99997636	20.00

3. The case of approximations of distributed-order differential operators via asymptotic expansion and GLT momentary symbols. In this last section we focus on the matrix sequences arising from the numerical approximation of a partial differential fractional operator. We recall that fractional-order differential equations have received tremendous attention in the last years for their ability to model anomalous diffusion phenomena (see [12, 13, 15, 16] and the references therein). Among them a new direction is represented by distributed-order equations (see, e.g., [1] and references therein). More specifically, the following model equation is considered, in which the fractional order is distributed via a definite integral:

$$(3.1) \quad \begin{cases} \frac{\partial u(x, t)}{\partial t} = \int_1^2 \rho(\alpha) \frac{\partial u^\alpha(x, t)}{\partial |x|^\alpha} d\alpha + f(x, t), & (x, t) \in \Omega = [a, b] \times [0, T], \\ u(x, 0) = u_0(x), & x \in (a, b), \\ u(a, t) = u(b, t) = 0, & t \in (0, T], \end{cases}$$

where $\rho(\alpha)$ is the kernel function that satisfies

$$\rho(\alpha) \geq 0, \quad 0 < \int_1^2 \rho(\alpha) c(\alpha) < \infty, \quad c(\alpha) = -\frac{1}{2 \cos(\frac{\alpha\pi}{2})} > 0,$$

while $f(x, t)$ is the source term and $\frac{\partial^\alpha u(x, t)}{\partial |x|^\alpha}$ is the Riesz fractional derivative of order $1 < \alpha < 2$ with respect to x defined as

$$\frac{\partial^\alpha u(x, t)}{\partial |x|^\alpha} = c(\alpha) ({}_a D_x^\alpha u(x, t) + {}_x D_b^\alpha u(x, t)).$$

The left-sided and right-sided Riemann-Liouville fractional derivatives ${}_a D_x^\alpha u(x, t)$, ${}_x D_b^\alpha u(x, t)$ are in turn defined as

$$\begin{aligned}
 {}_a D_x^\alpha u(x, t) &= \frac{1}{\Gamma(2-\alpha)} \frac{d^2}{dx^2} \int_a^x (x-y)^{1-\alpha} u(y, t) dy, \\
 {}_x D_b^\alpha u(x, t) &= \frac{1}{\Gamma(2-\alpha)} \frac{d^2}{dx^2} \int_x^b (y-x)^{1-\alpha} u(y, t) dy,
 \end{aligned}$$

where $\Gamma(\cdot)$ is the gamma function. As done in [1], we adopt a second-order finite difference method to discretize (3.1). Let n, m, l be positive integers, $h = \frac{b-a}{n+1}$ be the spatial width, $\Delta t = \frac{T}{m}$ be the time step size, $\Delta\alpha = \frac{1}{m}$ be the fractional step size, and consider the partition

$$x_i = a + ih, \quad i = 0, 1, \dots, n+1, \quad t_j = j\Delta t, \quad j = 0, 1, \dots, m.$$

Furthermore, we divide the interval $(1, 2)$ into l uniform subintervals and denote by $\Delta\alpha$ the length of such subintervals. The midpoint of each subinterval is given by $\alpha_k = 1 + (k - \frac{1}{2})\Delta\alpha$, $k = 1, 2, \dots, l$.

In particular, the matrices under consideration take the form

$$(3.2) \quad \frac{h^{\alpha_\ell}}{\Delta\alpha} \mathcal{T}_n = c_\ell T_n(g_{\alpha_\ell}) + c_{\ell-1} h^{\Delta\alpha} T_n(g_{\alpha_{\ell-1}}) + \dots + c_1 h^{\Delta\alpha(\ell-1)} T_n(g_{\alpha_1}),$$

where ℓ is a positive integer, all the coefficients c_j are positive, independent of n , and contained in a specific positive range $[c_*, c^*]$ (see [26, Proposition 3.8, Corollary 3.11] for the details concerning the matrices and the related generating functions). More importantly, all the functions g_{α_ℓ} are globally continuous, monotonically increasing in the interval $[0, \pi]$, and even in the whole definition domain $[-\pi, \pi]$.

The goal is to exploit the notion of GLT momentary symbols and use it in combination with the asymptotic expansions derived in a quite new research line (see [19] and the references therein) in order to have a very precise description of the spectrum of such matrices.

Indeed, under specific assumptions on the generating function f and fixing an integer $\nu \geq 0$, it is possible to give an accurate description of the eigenvalues of $T_n(f)$ via the following asymptotic expansion:

$$\lambda_j(T_n(f)) = w_0(\theta_{j,n}) + h w_1(\theta_{j,n}) + h^2 w_2(\theta_{j,n}) + \dots + h^\nu w_\nu(\theta_{j,n}) + E_{j,n,\nu},$$

where the eigenvalues of $T_n(f)$ are arranged in ascending order, $h = \frac{1}{n}$, and $\theta_{j,n} = \frac{j\pi}{n} = j\pi h$, for $j = 1, \dots, n$, and $E_{j,n,\nu} = O(h^{\nu+1})$ is the error. Moreover, $\{w_k\}_{k=1,2,\dots}$ is a sequence of functions from $[0, \pi]$ to \mathbb{R} . The idea of such procedure is that a numerical approximation of the value $w_k(\theta_{j,n})$ can be obtained by fast interpolation-extrapolation algorithms (see [20] and references therein). In particular, choosing ν proper grids $\theta_{j,n_1}, \theta_{j,n_2}, \dots, \theta_{j,n_\nu}$ with $n \gg n_\nu > \dots > n_1$, an approximation of the quantities $\tilde{w}_k(\theta_{j,n}) \approx w_k(\theta_{j,n})$ can be obtained. In the Hermitian case, we find that \tilde{w}_0 coincides with the generating function.

Concerning the example in (3.2), the idea is to link the functions $\tilde{w}_k^{c_i g_{\alpha_i}}$, $k = 1, \dots, \nu$, associated with each $c_i g_{\alpha_i}$ with the GLT momentary symbols of $\frac{h^{\alpha_\ell}}{\Delta\alpha} \mathcal{T}_n$. More precisely, for $j = 1, \dots, n$, for a fixed ν , we approximate the eigenvalues of $\frac{h^{\alpha_\ell}}{\Delta\alpha} \mathcal{T}_n$ by

$$(3.3) \quad \lambda_j \left(\frac{h^{\alpha_\ell}}{\Delta\alpha} \mathcal{T}_n \right) \approx c_\ell g_{\alpha_\ell}(\theta_{j,n}) + \sum_{t=1}^{\nu} h^t \left(\tilde{w}_t^{\alpha_\ell}(\theta_{j,n}) + \sum_{i=\ell-1}^1 \tilde{w}_{t-1}^{\alpha_i}(\theta_{j,n}) h^{-(1-\Delta\alpha(\ell-i))} \right),$$

where, for the sake of notation, we denoted by $\tilde{w}_t^{\alpha_i}$ the approximation of the t th asymptotic expansion coefficient associated with $c_i g_{\alpha_i}$ and the term $\tilde{w}_0^{\alpha_i}$ coincides with the evaluations of $c_i g_{\alpha_i}$.

We highlight that the terms in brackets on the right-hand side of the equality act as possible asymptotic expansion coefficients associated with the GLT momentary symbols g_n of $\frac{h^{\alpha_\ell}}{\Delta\alpha} \mathcal{T}_n$. Note that formula (3.3) can be rewritten in compact form as

$$\lambda_j \left(\frac{h^{\alpha_\ell}}{\Delta\alpha} \mathcal{T}_n \right) \approx \sum_{t=1}^{\nu} h^t \left(\tilde{w}_t^{\alpha_\ell}(\theta_{j,n}) + \sum_{i=\ell}^1 \tilde{w}_{t-1}^{\alpha_i}(\theta_{j,n}) h^{-(1-\Delta\alpha(\ell-i))} \right).$$

Hence, it is easy to see that the GLT momentary symbols correspond to taking ν of the asymptotic expansion equal to 1.

In the following we consider the cases where $\ell = 2$, $\ell = 5$, and $\ell = n$ as in [26, Section 4] and confirm at least numerically the conjecture in (3.3) for a fixed $\nu = 4$.

3.1. Examples. For $\ell = 2$, $\Delta\alpha$ is $\frac{1}{2}$, and the matrix in (3.2) becomes

$$2h^{\alpha_2} \mathcal{T}_n = c_2 \mathcal{T}_n(g_{\alpha_2}) + c_1 h^{\frac{1}{2}} \mathcal{T}_n(g_{\alpha_1}),$$

where $\alpha_1 = \frac{5}{4}$ and $\alpha_2 = \frac{7}{4}$. Exploiting the procedure based on formula (3.3) with $\nu = 4$, we compute an approximation of the eigenvalues of $c_2 \mathcal{T}_n(g_{\alpha_2}) + c_1 h^{\frac{1}{2}} \mathcal{T}_n(g_{\alpha_1})$ by

$$c_2 g_{\alpha_2}(\theta_{j,n}) + h \left[\tilde{w}_1^{\alpha_2}(\tilde{\theta}_{j,n}) + h^{-\frac{1}{2}} c_1 g_{\alpha_1}(\theta_{j,n}) \right] + \sum_{t=2}^{\nu} h^t \left[\tilde{w}_t^{\alpha_2}(\theta_{j,n}) + h^{-\frac{1}{2}} \tilde{w}_{t-1}^{\alpha_1}(\theta_{j,n}) \right],$$

for $j = 1, \dots, n$. We consider the cases where $n = 100, 500, 1000$ using an initial grid with $n_1 = 10$ points, and we compare the aforementioned approximations with those obtained by the evaluations of the GLT and GLT momentary symbols associated with the sequence described by the matrices in (3.2).

In Figure 3.1 we can observe that the approximation of the spectrum obtained by computing the evaluations of the GLT momentary symbols is better than that provided by the evaluations $c_\ell g_{\alpha_\ell}(\theta_{j,n})$. Moreover, by combining the notions of GLT momentary symbols with the asymptotic expansion described before (see Figure 3.2), the approximation errors are significantly reduced for almost all the eigenvalues. Note that the particular shape of the asymptotic expansion error depends on the fact that in correspondence with the grid points θ_{j,n_t} , $t = 1, \dots, \nu$, the quantities $\tilde{w}_t^{\alpha_i}$ are calculated exactly by the extrapolation-interpolation procedure. Moreover, note that the accuracy of the approximation via the combination of GLT momentary symbols and spectral asymptotic expansion seems to decrease corresponding to the maximum eigenvalue. Actually, this behavior is expected from the theory of the asymptotic expansion. Indeed, it is a consequence of the fact that the involved symbols are not trigonometric polynomials, and in particular they become non-smooth when periodically extended on the real line.

Following the analogous procedure, we consider the case where $\ell = 5$ and $\ell = n$, which are associated with $\Delta\alpha = \frac{1}{5}$ and $\Delta\alpha = \frac{1}{n}$, respectively. In Figures 3.3 and 3.5 we plot the approximations of the eigenvalues given by the three presented strategies for $\ell = 5$ and $\ell = n$. Again, we obtain numerical confirmation that the combination of the notions of GLT momentary symbols and asymptotic expansion provides accurate results even for moderate sizes, as confirmed by the error plots in Figures 3.4 and 3.6, for $n = 100, 500, 1000$.

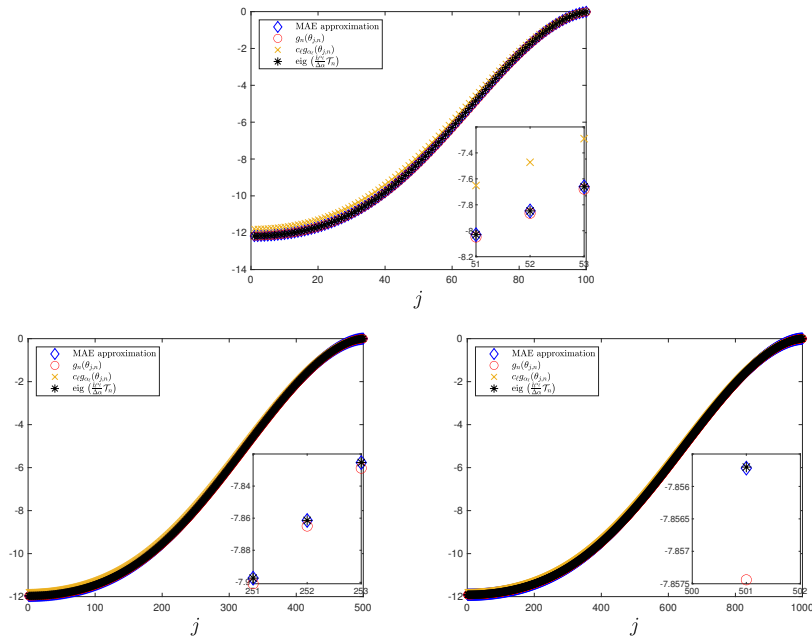


FIG. 3.1. Approximation of the eigenvalues of $\frac{h^{\alpha \ell}}{\Delta^{\alpha}} \mathcal{T}_n$, $\ell = 2$, by sampling the GLT and GLT momentary symbols and making use of the momentary asymptotic expansion (MAE) with $\nu = 4$, for $n = 100, 500, 1000$, with an initial grid of $n_1 = 10$ points.

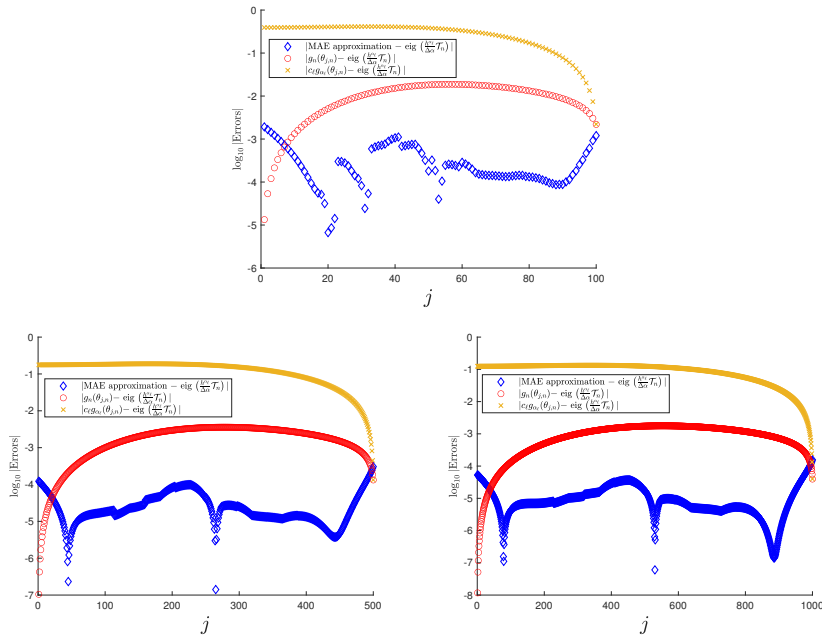


FIG. 3.2. Absolute errors of the approximation of the eigenvalues of $\frac{h^{\alpha \ell}}{\Delta^{\alpha}} \mathcal{T}_n$, $\ell = 2$, by sampling the GLT and GLT momentary symbols and making use of the momentary asymptotic expansion (MAE) with $\nu = 4$, for $n = 100, 500, 1000$, with an initial grid of $n_1 = 10$ points.

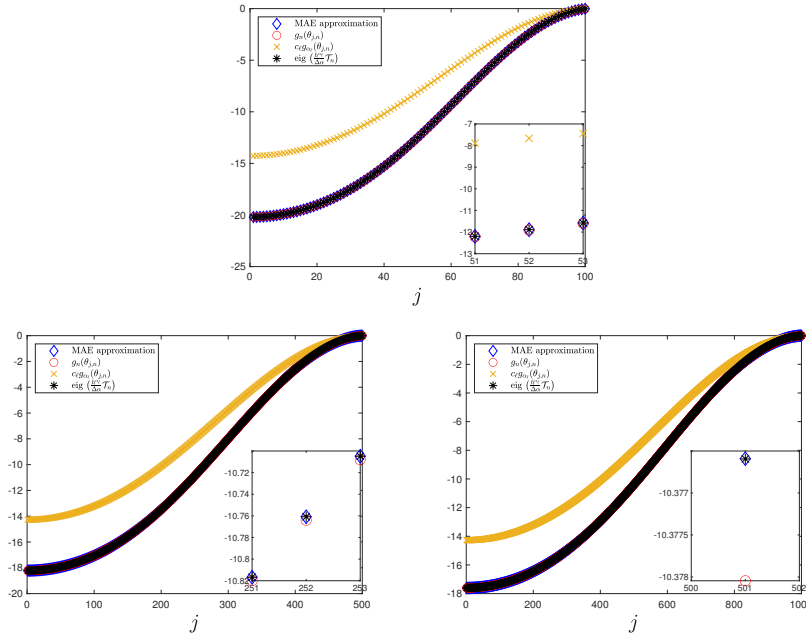


FIG. 3.3. Approximation of the eigenvalues of $\frac{h^{\alpha \ell}}{\Delta \alpha} T_n$, $\ell = 5$, by sampling the GLT and GLT momentary symbols and making use of the momentary asymptotic expansion (MAE) with $\nu = 4$, for $n = 100, 500, 1000$, with an initial grid of $n_1 = 10$ points.

The good outcome of the presented numerical tests gives ground to a finer analysis of the spectral features of the matrices considered in the case left open in [26]: indeed the analysis in [26] concerns the case where the integral partition width is given by a fixed value ℓ , independent of the space discretization step $h = \frac{b-a}{n+1}$, while in the present setting we consider the more difficult case in which the integral partition width is asymptotic to the adopted discretization step, that is, when in formula (3.2) we take $\alpha_k = 1 + (k - \frac{1}{2})\Delta\alpha$, $k = 1, 2, \dots, l$.

Moreover, efficient and fast algorithms which exploit the concept of momentary symbols can be studied for computing the singular values and eigenvalues of $T_n(f)$ with its possible block and variable coefficients generalizations, and this will be investigated in the future.

4. Concluding remarks. The main focus of this paper has been the characterization of the spectrum and the singular values of the coefficient matrix stemming from the approximation with space-time grids for a parabolic diffusion problem and from the approximation of distributed-order fractional equations. For this purpose we employed the classical GLT theory and the new concept of GLT momentary symbols. The first has permitted us to describe the singular value or eigenvalue asymptotic distribution of the sequence of the coefficient matrices. The latter has permitted us to derive a function able to describe the singular value or eigenvalue distribution of the matrix of the sequence, even for small matrix sizes, but under given assumptions. In particular, we exploited the notion of GLT momentary symbols, and we used it in combination with the interpolation-extrapolation algorithms based on the spectral asymptotic expansion of the involved matrices.

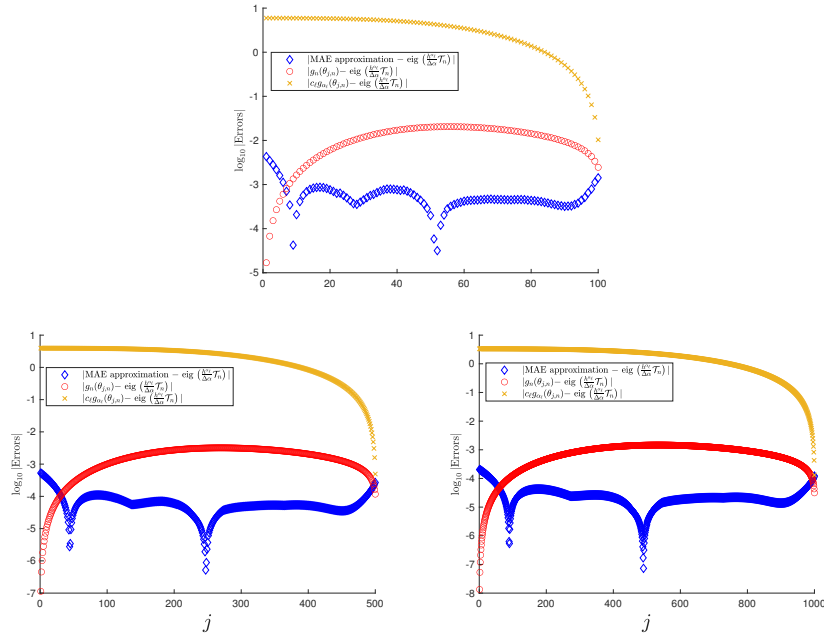


FIG. 3.4. Absolute errors of the approximation of the eigenvalues of $\frac{h^{\alpha} \ell}{\Delta \alpha} \mathcal{T}_n$, $\ell = 5$, by sampling the GLT and GLT momentary symbols and making use of the momentary asymptotic expansion (MAE) with $\nu = 4$, for $n = 100, 500, 1000$, with an initial grid of $n_1 = 10$ points.

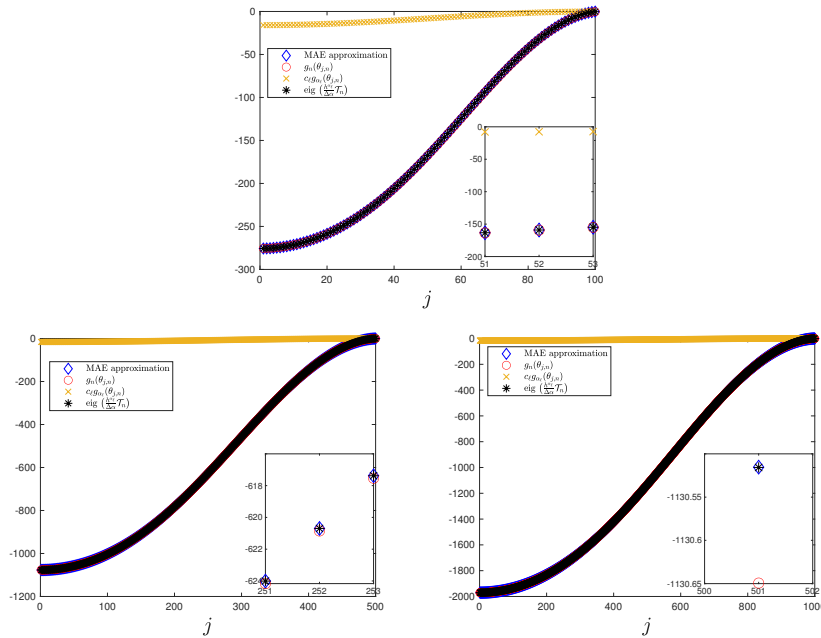


FIG. 3.5. Approximation of the eigenvalues of $\frac{h^{\alpha} \ell}{\Delta \alpha} \mathcal{T}_n$, $\ell = n$, by sampling the GLT and GLT momentary symbols and making use of the momentary asymptotic expansion (MAE) with $\nu = 4$, for $n = 100, 500, 1000$, with an initial grid of $n_1 = 10$ points.

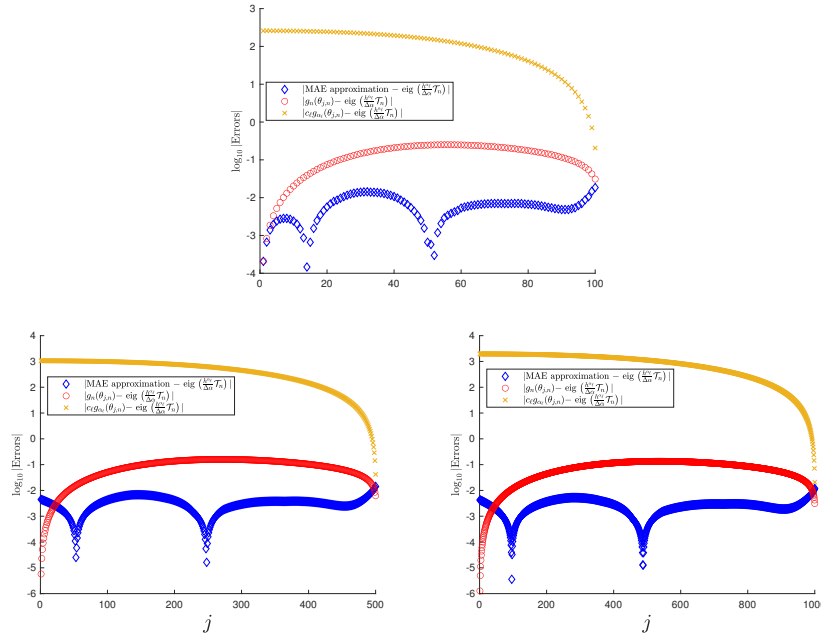


FIG. 3.6. Absolute errors of the approximation of the eigenvalues of $\frac{h^\alpha \ell}{\Delta \alpha} \mathcal{T}_n$, $\ell = n$, by sampling the GLT and GLT momentary symbols and making use of the momentary asymptotic expansion (MAE) with $\nu = 4$, for $n = 100, 500, 1000$, with an initial grid of $n_1 = 10$ points.

Many questions remain, and below we list some open problems to be considered in future research.

- More examples of the use of GLT momentary symbols in non-Toeplitz settings.
- The application of GLT momentary symbol in a pure Toeplitz setting but of very involved nature, like that expressed in relation (3.2). The use of GLT momentary symbol for the analysis of efficient iterative solvers, also of multigrid type, of linear systems, as those appearing in (2.1) also with the inclusion of variable coefficients.

Acknowledgment. This work was partially supported by INdAM-GNCS. Moreover, the work of Isabella Furci was also supported by the Young Investigator Training Program 2020 (YITP 2019) promoted by ACRI.

REFERENCES

- [1] M. ABBASZADEH, *Error estimate of second-order finite difference scheme for solving the Riesz space distributed-order diffusion equation*, Appl. Math. Lett., 88 (2019), pp. 179–185.
- [2] F. AVRAM, *On bilinear forms in Gaussian random variables and Toeplitz matrices*, Probab. Theory Related Fields, 79 (1988), pp. 37–45.
- [3] G. BARBARINO, C. GARONI, AND S. SERRA-CAPIZZANO, *Block generalized locally Toeplitz sequences: theory and applications in the unidimensional case*, Electron. Trans. Numer. Anal., 53 (2020), pp. 28–112. <https://etna.ricam.oeaw.ac.at/vol.53.2020/pp28-112.dir/pp28-112.pdf>
- [4] G. BARBARINO, C. GARONI, AND S. SERRA-CAPIZZANO, *Block generalized locally Toeplitz sequences: theory and applications in the multidimensional case*, Electron. Trans. Numer. Anal., 53 (2020), pp. 113–216. <https://etna.ricam.oeaw.ac.at/vol.53.2020/pp113-216.dir/pp113-216.pdf>
- [5] G. BARBARINO AND S. SERRA-CAPIZZANO, *Non-Hermitian perturbations of Hermitian matrix-sequences and applications to the spectral analysis of the numerical approximation of partial differential equations*, Numer. Linear Algebra Appl., 27 (2020), Art. e2286, 31 pages.

- [6] R. BHATIA, *Matrix Analysis*, Springer, New York, 1997.
- [7] M. BOLTEN, S-E. EKSTRÖM, I. FURCI, AND S. SERRA-CAPIZZANO, *Toeplitz momentary symbols: definition, results, and limitations in the spectral analysis of structured matrices*, *Linear Algebra Appl.*, 651 (2022), pp. 51–82.
- [8] E. BOZZO AND C. DI FIORE, *On the use of certain matrix algebras associated with discrete trigonometric transforms in matrix displacement decomposition*, *SIAM J. Matrix Anal. Appl.*, 16 (1995), pp. 312–326.
- [9] H. BREZIS, *Functional Analysis, Sobolev Spaces and Partial Differential Equations*, Springer, New York, 2011.
- [10] R. CHAN AND X. JIN, *An Introduction to Iterative Toeplitz Solvers*, SIAM, Philadelphia, 2007.
- [11] G. CALCAGNI, *Towards multifractional calculus* *Front. Phys.*, 6 (2018), 6 pages.
- [12] M. CAPUTO, *Diffusion with space memory modelled with distributed order space fractional differential equations*, *Ann. Geophys.*, 46 (2003), pp. 223–234.
- [13] M. CAPUTO AND M. FABRIZIO, *The kernel of the distributed order fractional derivatives with an application to complex materials*, *Fractal Fract.*, 1 (2017), 11 pages.
- [14] T. CECCHERINI-SILBERSTEIN, F. SCARABOTTI, AND F. TOLLI, *Harmonic Analysis on Finite Groups*, Cambridge University Press, Cambridge, 2008.
- [15] W. DENG, B. LI, W. TIAN, AND P. ZHANG, *Boundary problems for the fractional and tempered fractional operators*, *Multiscale Model. Simul.*, 16 (2018), pp. 125–149.
- [16] W. DING, S. PATNAIK, S. SIDHARDH, AND F. SEMPERLOTTI, *Applications of distributed-order fractional operators: a review*, *Entropy*, 23 (2021), Article 110, 42 pages.
- [17] M. DONATELLI, M. MAZZA, AND S. SERRA-CAPIZZANO, *Spectral analysis and structure preserving preconditioners for fractional diffusion equations*, *J. Comput. Phys.*, 307 (2016), pp. 262–279.
- [18] ———, *Spectral analysis and multigrid methods for finite volume approximations of space-fractional diffusion equations*, *SIAM J. Sci. Comput.* 40 (2018), pp. A4007–A4039.
- [19] S.-E. EKSTRÖM, I. FURCI, AND S. SERRA-CAPIZZANO, *Exact formulae and matrix-less eigensolvers for block banded symmetric Toeplitz matrices*, *BIT*, 58 (2018), pp. 937–968.
- [20] S.-E. EKSTRÖM, AND C. GARONI, *A matrix-less and parallel interpolation–extrapolation algorithm for computing the eigenvalues of preconditioned banded symmetric Toeplitz matrices*, *Numer. Algorithms*, 80 (2019), pp. 819–848.
- [21] S.-E. EKSTRÖM, C. GARONI, A. JOZEFIAK, AND J. PERLA, *Eigenvalues and eigenvectors of tau matrices with applications to Markov processes and economics*. *Linear Algebra Appl.*, 627 (2021), pp. 41–71.
- [22] C. ESTATICO AND S. SERRA-CAPIZZANO, *Superoptimal approximation for unbounded symbols*, *Linear Algebra Appl.*, 428 (2008), pp. 564–585.
- [23] C. GARONI AND S. SERRA-CAPIZZANO, *Generalized Locally Toeplitz Sequences: Theory and Applications. Vol 1*, Springer, Cham, 2017.
- [24] ———, *Generalized Locally Toeplitz Sequences: Theory and Applications. Vol 2*, Springer, Cham, 2018.
- [25] U. GRENANDER AND G. SZEGŐ, *Toeplitz Forms and Their Applications*, 2nd ed., Chelsea, New York, 1984.
- [26] M. MAZZA, S. SERRA-CAPIZZANO, AND M. USMAN, *Symbol-based preconditioning for Riesz distributed-order space-fractional diffusion equations*, *Electron. Trans. Numer. Anal.*, 54 (2021), pp. 499–513.
<https://etna.ricam.oeaw.ac.at/vol.54.2021/pp499-513.dir/pp499-513.pdf>
- [27] M. K. NG, *Iterative Methods for Toeplitz Systems*, Oxford University Press, New York, 2004.
- [28] S. V. PARTER, *On the distribution of the singular values of Toeplitz matrices*, *Linear Algebra Appl.*, 80 (1986), pp. 115–130.
- [29] M. A. POZIO AND A. TESEI, *On the uniqueness of bounded solutions to singular parabolic problems*, *Discrete Contin. Dyn. Syst.*, 13 (2005), pp. 117–137.
- [30] S. SERRA-CAPIZZANO, D. BERTACCINI, AND G. H. GOLUB, *How to deduce a proper eigenvalue cluster from a proper singular value cluster in the nonnormal case*, *SIAM J. Matrix Anal. Appl.*, 27 (2005), pp. 82–86.
- [31] A. TESEI AND F. PUNZO, *Uniqueness of solutions to degenerate elliptic problems with unbounded coefficients*, *Ann. Inst. H. Poincaré C Anal. Non Linéaire*, 26 (2009), pp. 2001–2024.
- [32] P. TILLI, *A note on the spectral distribution of Toeplitz matrices*, *Linear and Multilinear Algebra*, 45 (1998), pp. 147–159.
- [33] E. TYRTYSHNIKOV AND N. ZAMARASHKIN, *Spectra of multilevel Toeplitz matrices: advanced theory via simple matrix relationships*, *Linear Algebra Appl.*, 270 (1998), pp. 15–27.
- [34] N. ZAMARASHKIN AND E. TYRTYSHNIKOV, *Distribution of the eigenvalues and singular numbers of Toeplitz matrices under weakened requirements on the generating function*. *Sb. Mat.*, 188 (1997), pp. 1191–1201.
- [35] A. ZYGMUND, *Trigonometric Series*, Cambridge University Press, New York, 1959.